Probing the Role of the Chloride Ion in the Mechanism of Human Pancreatic α-Amylase[†,‡]

Shin Numao,[§] Robert Maurus,[||] Gary Sidhu,[||] Yili Wang,[||] Christopher M. Overall,[||,⊥] Gary D. Brayer,[||] and Stephen G. Withers*[,§,||]

Department of Chemistry, University of British Columbia, Vancouver, British Columbia, Canada V6T 1Z1, and Department of Biochemistry and Molecular Biology and Department of Oral Biological and Medical Sciences, University of British Columbia, British Columbia, Canada V6T 1Z3

Received July 26, 2001; Revised Manuscript Received October 22, 2001

ABSTRACT: Human pancreatic α-amylase (HPA) is a member of the α-amylase family involved in the degradation of starch. Some members of this family, including HPA, require chloride for maximal activity. To determine the mechanism of chloride activation, a series of mutants (R195A, R195Q, N298S, R337A, and R337Q) were made in which residues in the chloride ion binding site were replaced. Mutations in this binding site were found to severely affect the ability of HPA to bind chloride ions with no binding detected for the R195 and R337 mutant enzymes. X-ray crystallographic analysis revealed that these mutations did not result in significant structural changes. However, the introduction of these mutations did alter the kinetic properties of the enzyme. Mutations to residue R195 resulted in a 20−450-fold decrease in the activity of the enzyme toward starch and shifted the pH optimum to a more basic pH. Interestingly, replacement of R337 with a nonbasic amino acid resulted in an α-amylase that no longer required chloride for catalysis and has a pH profile similar to that of wild-type HPA. In contrast, a mutation at residue N298 resulted in an enzyme that had much lower binding affinity for chloride but still required chloride for maximal activity. We propose that the chloride is required to increase the pK_a of the acid/base catalyst, E233, which would otherwise be lower due to the presence of R337, a positively charged residue.

α-Amylase (α-1,4-glucan-4-glucanohydrolase, EC 3.2.1.1) is an endoglycosidase that catalyzes the hydrolysis of α-(1,4)-glycosidic bonds of glucose polymers with net retention of anomeric configuration. Because such polymers are widely used as an energy source in nature, it is not surprising that α-amylases are produced by various organisms ranging from microorganisms to mammals (*1*, *2*). From sequence analysis, this group of glycosidases has been assigned to family 13 of Henrissat's glycosidase classification (*3*−*6*). Enzymes of this family, which also includes enzymes such as α-glucosidases, cyclodextrin glucanotransferases, pullulanases, and glycogen debranching enzyme, have significant sequence similarity in only four short regions, each consisting of about 20 amino acids.

Recently, the three-dimensional structures of a number of α-amylases have been determined and published, including those from *Alteromonas halioplanctis* (*7*), *Aspergillus oryzae* (*8*), *Aspergillus niger* (*9*), *Bacillus licheniformis* (*10*), barley (*11*), porcine pancreas (*12*), human saliva (*13*), and human pancreas (*14*). Despite relatively weak similarities in the primary structures, the tertiary structures are fairly well conserved within this group of enzymes. In general, α-amylases are monomeric proteins of about 50 kDa with three structural domains. Domain A is an α/*β* barrel that contains the active site. Domain B consists of a loop that protrudes from domain A and forms the conserved calcium ion binding site. These two domains closely interact via the bound calcium ion. Domain C is an eight-stranded *β*-barrel-type structure at the C-terminus. This latter domain is only loosely associated with the other two domains, and its function is still not understood.

Evidence from NMR (*15*), mutagenic (*16*), and structural studies (*8*, *17*) has suggested that α-amylases catalyze hydrolysis by the double displacement mechanism of retaining glycosidases (Figure 1) (*18*−*20*). In this mechanism, a covalent glycosyl-enzyme intermediate forms as a consequence of a nucleophilic displacement of the aglycon by a catalytic carboxylic acid (D197; human pancreatic α-amylase numbering will be used throughout the paper unless otherwise noted). The covalent intermediate is then hydrolyzed through another nucleophilic displacement, this time by a water molecule, to result in the release of the product with net retention of configuration at the anomeric carbon. Both the glycosylation and deglycosylation steps are thought to proceed through oxocarbenium ion-like transition states. These transition states are stabilized by another active site carboxylic acid that acts first as a general acid and then as a general base catalyst.

[†] This work was funded by the Canadian Institutes of Health Research (CIHR). S.N. is the recipient of a CIHR Studentship. G.S. is the recipient of an NSERC Postgraduate Scholarship. C.M.O. is funded by a Scientist Award from the CIHR.

[‡] Coordinates for the structures described in this work have been deposited in the Protein Data Bank (ID codes 1KB3, 1KGX, 1KGU, and 1KGW).

* To whom correspondence should be addressed. Tel: 604-822-3402. Fax: 604-822-8867. E-mail: withers@chem.ubc.ca.

[§] Department of Chemistry, University of British Columbia.

[||] Department of Biochemistry and Molecular Biology, University of British Columbia.

[⊥] Department of Oral Biological and Medical Sciences, University of British Columbia.

10.1021/bi0115636 CCC: $22.00
Published on Web 12/05/2001

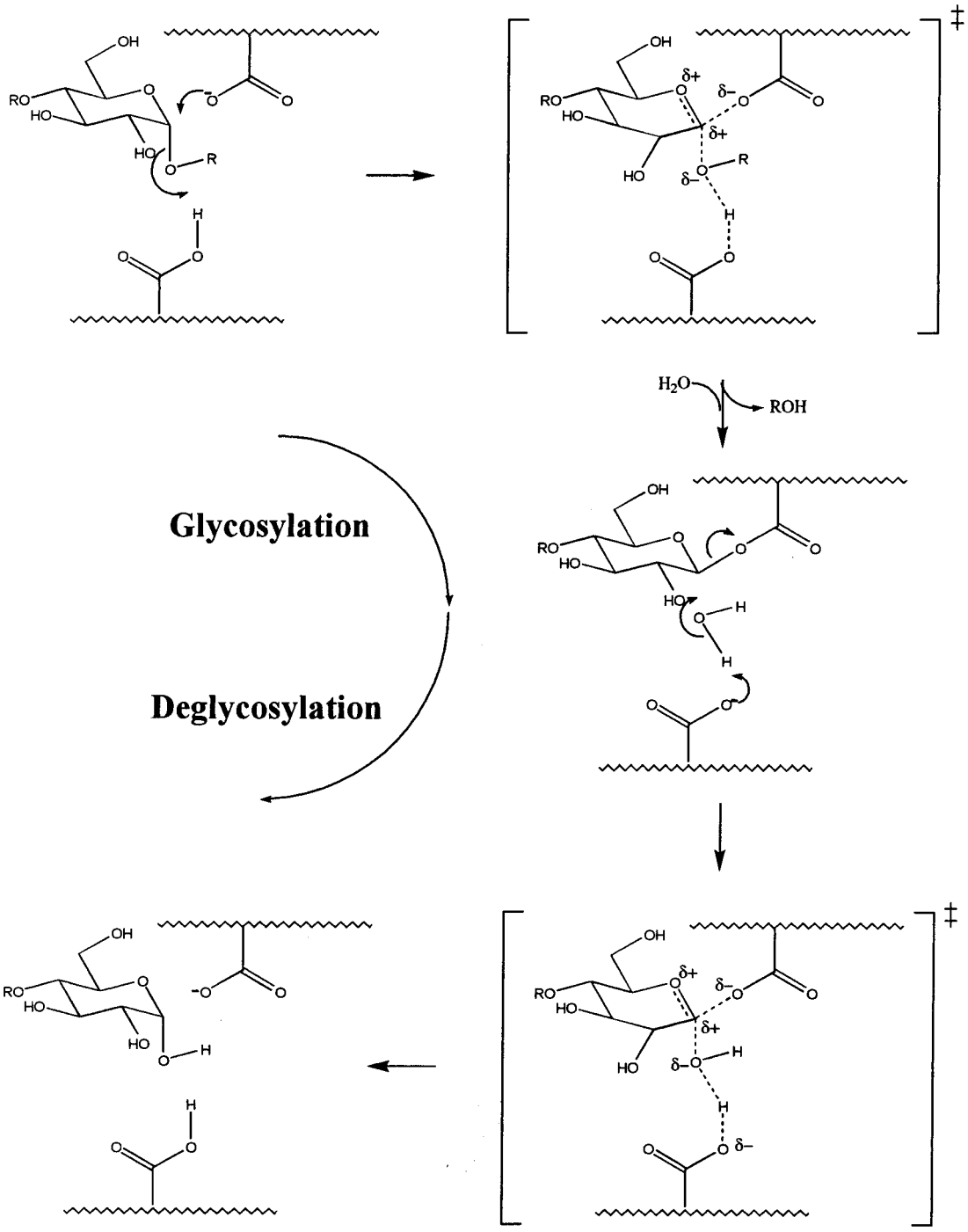

FIGURE 1: Proposed mechanism for HPA. R = α-(1,4)-glucosyl chain.

Several α-amylases, including the porcine pancreatic enzyme (*21*) and the bacterial enzyme from *A. halioplanctis* (*22*), have been shown to require chloride for full catalytic activity. In these α-amylases, the removal of chloride resulted in not only a significant decrease in activity but also a shift in pH optima (*22*, *23*). In contrast, most microbial α-amylases are not affected by the presence of chloride (*2*). This allows α-amylases to be classified as either chloride-dependent or chloride-independent enzymes (*24*). Recent structural determinations have shown that, in these chloride-dependent α-amylases, there is a conserved chloride ion binding site (Figure 2) located in domain A consisting of three residues, R195, N298, and R337 (sometimes lysine) (*14*). These residues coordinate a chloride ion, positioning it ~5 Å away from the active site residues. Of these three residues, the R195 and N298 are almost completely conserved in both groups of α-amylases. The fact that these residues are conserved even though there is no chloride ion binding site in some cases does not come as too much of a surprise since R195 is involved in key H-bonding interactions with several catalytic residues while N298 seems to be involved in stabilizing a key active site loop. In contrast, R337 is conserved only within the chloride-dependent α-amylases: in the chloride-independent α-amylases, this residue is replaced by a nonbasic amino acid.

Physiologically, human pancreatic α-amylase (HPA)[1] plays an important role in the digestion of dietary starch with inhibition of this enzyme resulting in the reduction of

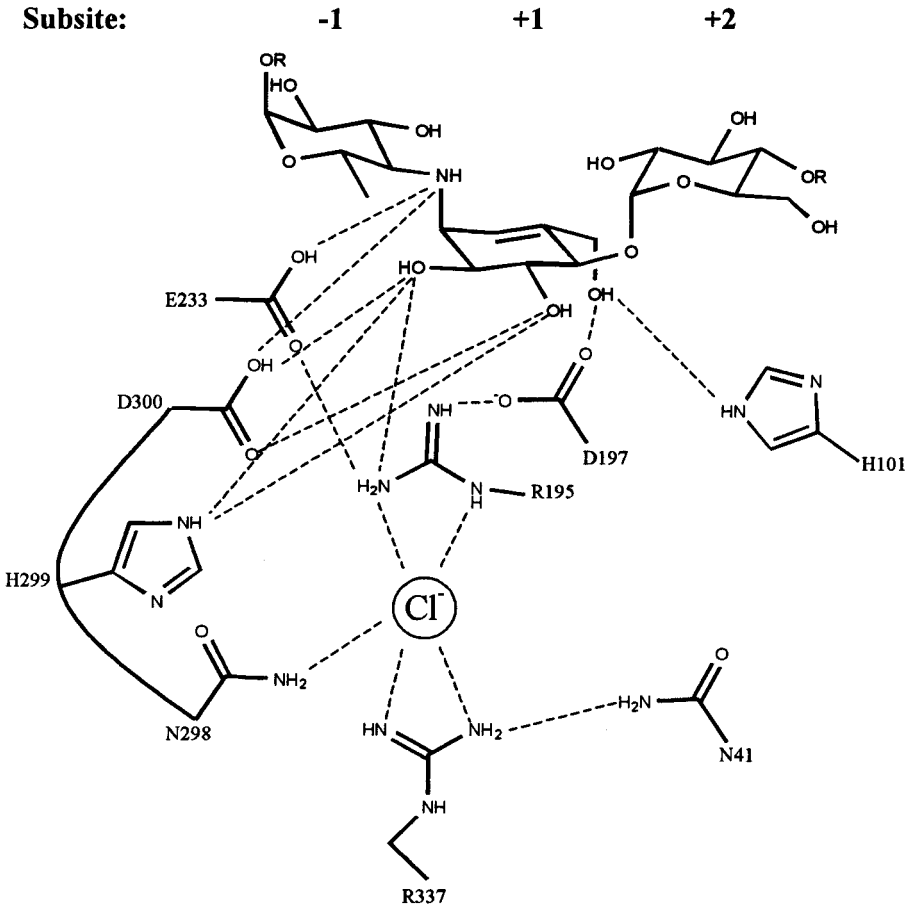

FIGURE 2: Diagram of some representative interactions between the chloride ion binding site residues, the active site residues, and the inhibitor, acarbose in HPA (*31*). Dashed lines represent distances shorter than 3.5 Å.

postprandial blood glucose levels (*25*−*27*). Control of blood glucose levels through modulation of α-amylase activities therefore has therapeutic implications for diseases such as diabetes and obesity. Indeed, at least one drug (acarbose) that works in this way is currently commercially available. Since chloride is also able to modulate the activity of HPA, the study of the chloride ion binding site may allow for insights into the design of potential new inhibitors of this enzyme. To gain further understanding of the mechanism by which the chloride ion is modulating the α-amylase activity, R195, N298, and R337 of HPA were mutated and the gene products subjected to structural and mechanistic analysis. The results of such studies are presented in this report.

EXPERIMENTAL PROCEDURES

Materials. All buffer salts were obtained from Fisher Scientific Canada and contained less than 0.005% chloride. All other chemicals were obtained from Sigma Chemical Co. unless otherwise noted.

Bacterial Strain, Media, and Plasmids. Escherichia coli DH5α subcloning efficiency competent cells were obtained from Gibco BRL Products and were used for all transformations and DNA manipulations according to standard procedures (*28*). *Pichia pastoris* strain GM5011 was used for the expression of proteins. Growth and expression media were prepared as published in the *Pichia* expression kit (Invitrogen). The construction of the *E. coli*−*P. pastoris* shuttle vector (pPIC9-AMY) containing the HPA gene under control of the AOX1 promoter has been published previously (*16*).

Site-Directed Mutagenesis. Single codon mutations were introduced to the HPA gene using the QuikChange site-directed mutagenesis kit (Stratagene) and GeneAmp PCR system 2400 (Perkin-Elmer). The primers used for mutagenesis were as follows (mutations introduced are underlined): CATTGGTGTTGCAGGGTTCGCACTTGATGCTTCCAAGCAC and GTGCTTGGAAGCATCAAGTGCGAACCCTGCAACACCAATG for R195A; CATTGGTGTTGCAGGGTTCCAACTTGATGCTTCCAAGCAC and GTGCTTGGAAGCATCAAGTTGGAACCCTGCAACACCAATG for R195Q; CTCGTTGATTGTCATGGCTATCCACAAAGACAA and CTTGTCTTTGTGGATAGCCATGACAATCAAGGA for N298S; CATCCTTACGGATTTACAGCAGTAATGTCAAGCTACCGTTGG and CCAACGGTAGCTTGACATTACTGCTGTAAATCCGTAAGGATC for R337A; and CATCCTTACGGATTTACACAGGTAATGTCAAGCTACCGTTGG and CCAACGGTAGCTTGACATTACCTGTGTAAATCCGTAAGGATG for R337Q.

All primers were chemically synthesized at the Nucleic Acid and Protein Services (NAPS) Unit at the University of British Columbia (Vancouver, Canada). All mutations were confirmed by sequencing of the entire HPA cDNA, carried out by the NAPS Unit.

Protein Expression and Purification. Transformation of mutated pPIC9-AMY plasmids into *P. pastoris* cells and

[1] Abbreviations: HPA, human pancreatic α-amylase; ESI-MS, electrospray ionization mass spectrometry.

subsequent selection were carried out according to directions in the *Pichia* expression kit (Invitrogen). Cultures (total volume of 3 L) were incubated in buffered glycerol complex media at 30 °C for 1 day. After a 5-fold concentration by centrifugation, the medium was changed to buffered methanol complex medium to induce protein expression. The cultures were incubated at 30 °C for 2 days with addition of 50% methanol to a final concentration of 0.5% (v/v) every 12 h. The cells were removed from the supernatant by centrifugation followed by filtration through a 0.45 μm filter (Gelman). Wild-type and mutant HPAs were deglycosylated and then purified by passing the medium though a phenyl-Sepharose column followed by a Q-Sepharose column (Pharmacia) as published previously (*16*). The mass and purity of the purified proteins obtained were confirmed by ESI-MS and SDS−PAGE. Extensive buffer exchange against 5 mM phosphate buffer, pH 7.0, was done on the wild-type and mutant HPAs by centrifugal ultrafiltration using Amicon Centripreps to remove any residual chloride.

Kinetic Assays. α-Amylase activities for the wild-type and mutant enzymes were determined in 50 mM sodium phosphate buffer, pH 6.9 at 30 °C. Enzyme was added (final concentration of 90−630 nM) to a solution of 1% starch (w/v) and incubated for an appropriate length of time, depending on the activity of the enzyme. The enzyme reaction was stopped using an equal volume of stop solution (4.4 mM 3,5-dinitrosalicylic acid, 1 M sodium potassium tartrate, 0.4 M NaOH). The increase in reducing sugar was determined by boiling this reaction mix for 6 min and measuring the absorption at 546 nm using a UNICAM UV/vis spectrophotometer (*29*). Each point was done in duplicate, and the average of the two values was reported. All activities are reported in millimolar maltose produced per second per millimolar α-amylase (s^{-1}) at 30 °C.

Chloride dependence of HPA activity was determined by measuring reaction rates at varying chloride concentrations (0−100 mM). The data (chloride concentration vs activity) were fit to a ligand binding equation by nonlinear regression using the program GraFit 4.09 (*30*).

The dependence of HPA activity on pH was determined by measuring the activities of the wild-type and mutant enzymes using the same conditions as above with the exception of the buffer: pH 5.6, 6.0, 6.5, 7.1, 7.6, 8.1, and 8.4 (sodium phosphate buffer) and pH 8.7, 9.6, and 10.2 (sodium carbonate buffer). The plot of pH vs activity was fit to a double ionization pH curve by nonlinear regression using the program GraFit 4.09.

The K_M values for starch were determined at various pH values using the above method at a series of starch concentrations [0.1%−1.58% (w/v)]. The data were fit to the Michaelis−Menten equation by nonlinear regression using the program GraFit 4.09.

Structure Determinations. Crystals of mutant HPAs were grown using conditions previously described (*31*). All crystallization, soaking and data collection procedures were conducted at room temperature. Diffraction data were collected on a Rigaku R-AXIS IIC imaging plate area detector system using Cu Kα radiation supplied by a Rigaku RU300 rotating anode generator operating at 50 kV and 100 mA. Intensity data were integrated, scaled, and reduced to structure factor amplitudes, with the HKL suite of programs (*32*). Data collection statistics are provided in Table 1. The results of diffraction data collections showed that the various mutant protein crystals examined were of two types. This phenomenon has been noted before in this system and appears to be linked to the extent of glycosylation at a site remote from the active site, as well as the nature of substitutions introduced into the polypeptide chain (*31*). For the first crystal type, comprising crystals from the R195A and R195Q mutant HPAs, unit cell parameters were found to be isomorphous with those of wild-type HPA (*16*). The second crystal type, found for R337A and R337Q mutant protein crystals, was isomorphous with that previously described for crystals of a D300N/acarbose complex (*31*).

Table 1: Summary of Structure Determination Statistics

	mutant structures studied			
	R195A	R195Q	R337A	R337Q
data collection parameters				
space group	$P2_12_12_1$	$P2_12_12_1$	$P2_12_12_1$	$P2_12_12_1$
unit cell dimensions (Å)				
a	52.95	53.05	53.06	52.94
b	68.79	69.03	74.98	74.93
c	131.93	131.83	137.11	137.05
total no. of measurements	328644	312384	285470	297678
no. of unique reflections	41336	32187	44090	29654
mean $I/\sigma I$[a]	18.9 (10.8)	16.4 (10.7)	19.4 (9.3)	17.3 (8.2)
multiplicity[a]	3.4 (2.1)	3.3 (2.6)	3.7 (1.9)	3.8 (2.2)
merging *R*-factor (%)[a]	4.6 (9.6)	6.5 (9.3)	7.1 (10.8)	5.6 (13.4)
maximum resolution (Å)	1.9	2.0	1.9	2.0
structure refinement values				
no. of reflections	27164	31572	36985	28198
resolution range (Å)	10−2.1	10−2.0	10.0−2.0	10−2.1
completeness within range (%)[b]	92 (86)	88 (73)	93 (87)	94 (84)
no. of protein atoms	3939	3944	3939	3944
no. of solvent atoms	238	261	220	171
av thermal factors (Å^2)				
protein atoms	17.1	20.4	20.9	22.6
solvent atoms	37.4	44.9	40.6	38.5
final crystallographic *R*-factor (%)	19.3	19.7	19.3	19.0
final structure stereochemistry				
rmsd, bonds (Å)	0.007	0.006	0.005	0.005
rmsd, angles (deg)	1.081	1.060	1.004	1.067

[a] Values in parentheses are for the highest resolution shell: 1.97−1.90 Å for the R195A and R337A mutant HPAs and 2.07−2.00 Å for the R195Q and R337Q mutant HPAs. [b] Values in parentheses are for the highest resolution shell: 2.07−2.00 Å for the R195Q and R337A mutant HPAs and 2.14−2.10 Å for the R195A and R337Q mutant HPAs.

Refinement of all structural models was accomplished with X-PLOR (*33*). In these analyses, cycles of simulated annealing, positional, and thermal *B* refinements, were alternated with manual model rebuilding with O (*34*). The complete polypeptide chain for all refinement models was examined periodically during this process with $F_o - F_c$, $2F_o - F_c$, and fragment-deleted difference electron density maps. During such examinations, the positions of substituted amino acids were determined, and solvent molecule peaks were assigned. The validity of solvent molecules was assessed on the basis of both hydrogen-bonding potential to protein atoms and the refinement of a thermal factor of <75 Å^2. An *N*-acetylglucosamine moiety was found bound to the side chain of N461 only in the structures of the R195A, R195Q, and R337Q mutant HPAs and was refined accordingly. Final refinement statistics for each structure determination are detailed in Table 1. Coordinate error, as estimated from a Luzzati plot (*35*), is 0.22, 0.22, 0.21, and 0.23 Å for the R195A, R195Q, R337A, and R337Q mutant structures, respectively.

Table 2: Key Hydrogen Bond Interaction Distances (Å) in the Chloride Binding Site of Wild-Type and Mutant HPAs[a]

protein/ residue	Cl/WAT	Q41	D96	Q195	D197	E233	N301	ACB
WT								
R195	3.23/3.34		2.86		2.92	3.48/3.51		
N298	3.38						3.01/*2.84*	
R337	3.14/3.45	2.71						
WT/ACB								
R195	3.21/3.39		2.84		2.88	3.50/3.77		2.94
N298	3.42						3.19/*2.86*	
R337	3.14/3.27	2.82						
R195A								
A195								
N298	3.23w						3.02/*2.68*	
R337	3.19/3.84w	2.96						
R195Q								
Q195	3.41w							
N298	3.23w						3.07/*2.73*	
R337	3.57/2.95w	2.85		2.91				
R337A								
R195	(4.93)w		2.91		3.08	2.97		
N298	(3.86)w						3.01/*2.84*	
A337								
R337Q								
R195	2.82w		2.85		3.24	2.80		
N298	3.47w						3.02/*2.76*	
Q337	(4.70)w	3.38						

[a] Distances italicized are side chain to main chain interactions. Interactions are to a water molecule if labeled with a w. The abbreviation ACB refers to the bound inhibitor acarbose (also see Figure 4).

RESULTS

Structural Studies of the Chloride Ion Binding Site

R195 Mutant HPA Structures. High-resolution studies have delineated the structural determinants and detailed interactions that form the chloride ion binding site in HPA (Table 2) (*14*). As shown in Figure 2, two residues playing a primary role in binding chloride ion are R195 and R337. It is notable that R195 is also directly hydrogen bonded to D197, a residue identified as the catalytic nucleophile (*16*), as well as to E233, a prime candidate to function as the acid/base catalyst (Figure 1). It has also been shown that R195 (along with H299 and D300) forms a hydrogen bond to the O2 hydroxyl group of the sugar residue bound in the −1 binding subsite that is attacked by the nucleophile during catalysis (*31*). In contrast, R337 is located further from the active site residues and forms the bottom of the chloride ion binding site. Its sole role appears to be in assisting chloride ion binding. The other amino acid that directly interacts with bound chloride ion is N298.

Substitution of R195 with an alanine causes little perturbation of the main chain conformation of HPA. It does, however, lead to the loss of the ability of HPA to bind chloride ion, and a water molecule is found at this position instead (Figure 3a). The effect of removal of the side chain of R195 and the consequent loss of the chloride ion is a shift of H299 away from this region and a shift of E233 toward the newly opened space within the active site region. Notably, the other major chloride ion ligand, R337, exhibits minimal movement in this mutant HPA.

Of the two active site water molecules, the one that had been earlier identified as potentially participating in the acid/base catalytic step (*31*) is still present in the R195A HPA. The second, normally located at the expected O2 hydroxyl position of the substrate sugar ring located in the −1 binding subsite, is not present. This absence of the second water is not too surprising since R195 is a key ligand to the water in the wild-type enzyme.

Surprisingly, in the R195A mutant protein no significant movement is observed in the side chain of the catalytic nucleophile D197, suggesting that the interaction between the side chain of R195 does not play a key role in orienting the side chain of D197 for catalysis. Figure 4 illustrates the close juxtaposition of the chloride ion binding site and its major ligands to the position of the bound inhibitor acarbose in wild-type HPA. Notable in this enzyme−inhibitor complex is the central positioning of the side chain of R195, which interacts with almost all of the major catalytic elements, the bound inhibitor, and the bound chloride ion. The closest approach of bound inhibitor atoms to the chloride ion is 5.6 Å.

In the R195Q HPA, the shorter glutamine side chain follows a course similar to that of the original arginine group, but of course this substitution does lead to more open space in the vicinity of the chloride ion binding site and adjacent to the catalytic residues (Figure 3b). As is the case with the R195A HPA, no significant movement in the side chain of R337 is noted when R195 is substituted with a glutamine. Despite favorable positioning of the end of the Q195 side chain to possibly hydrogen bond to a chloride ion, a water molecule is found at the location of the normally bound chloride ion just as was seen in the R195A HPA. This demonstrates the importance of the charged interaction between bound chloride ion and the side chain of R195, which cannot apparently be replaced with a hydrogen bond. In response to the more open space generated, movements similar to that of R195A are noted for the side chains of H299 and E233 in the R195Q HPA. A unique feature of the R195Q HPA is the displacement of both the active site water molecules discussed earlier. In their place is found a single water molecule at an alternative position that is found to interact with all of H299, E233, D197, and D300.

R337 Mutant HPA Structures. Overall, replacement of R337 with an alanine causes little perturbation of the structure of HPA, other than the loss of chloride ion (Figure 3c,d). Interestingly, nothing is found bound at the normal chloride ion binding site, although, once again, a new water molecule is observed at the position formally occupied by the extremity of the originally resident R337. Only very slight changes are observed for the side chains of R195, E233, H299, and D300. The two active site water molecules previously discussed also retain their positions in the R337A HPA. It is remarkable that so little structural change has occurred in this mutant despite the removal of a large, charged, and internal side chain, as well as an internally bound chloride ion.

Substitution of R337 with glutamine also has little impact on the structure of HPA, other than the loss of chloride ion and slight shifts observed for the positions of R195, E233, H299, and D300. The shorter side chain of Q337 is found oriented approximately like that of the longer R337 in wild-type HPA. One feature unique to the R337Q HPA is the observed water structure. As with the R337A HPA, a new water molecule is found at the position previously occupied by the end of the arginine side chain, but surprisingly, an additional water molecule is observed at the position oc-

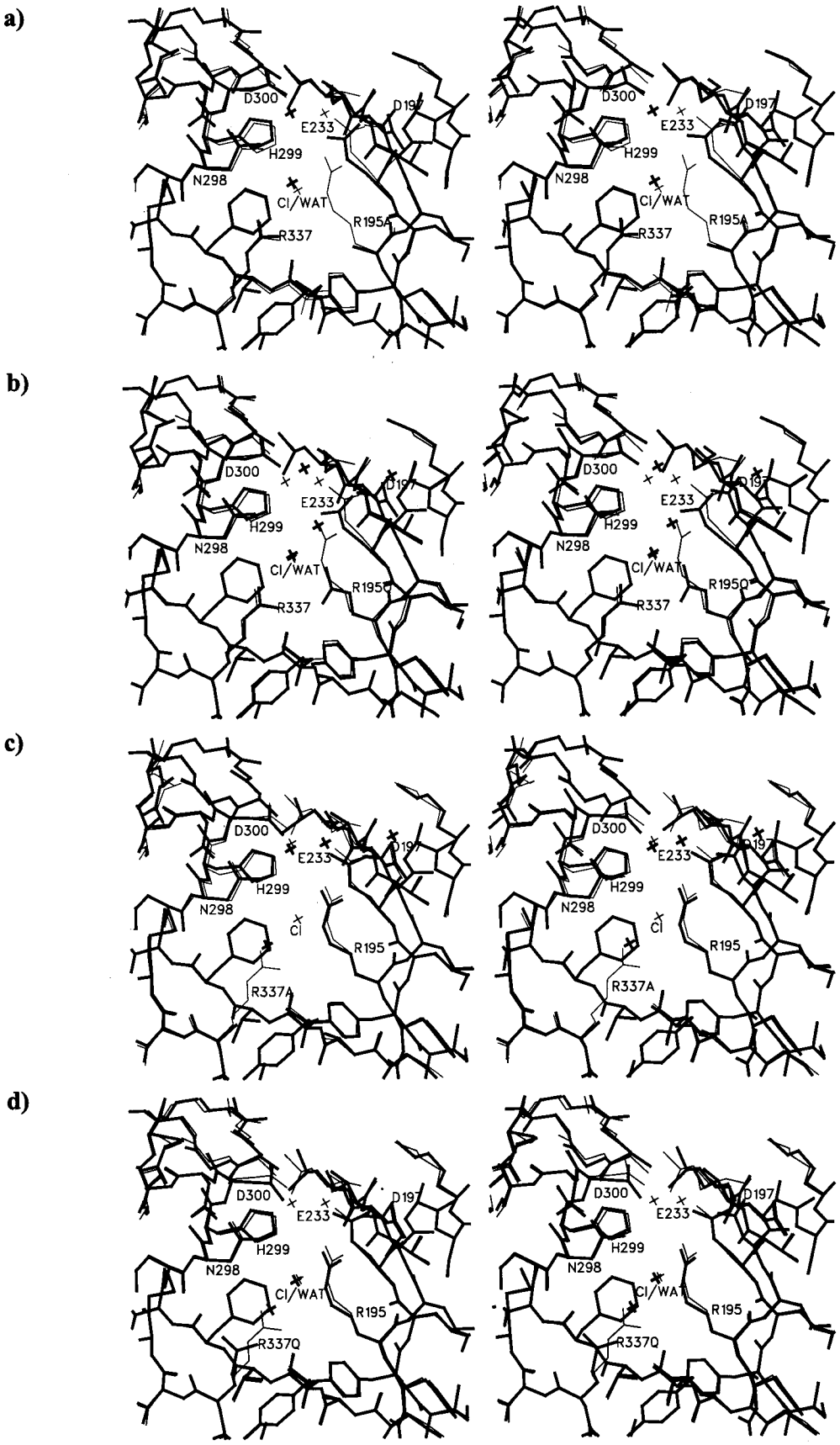

FIGURE 3: Stereo plots of the chloride ion binding site in the (a) R195A, (b) R195Q, (c) R337A, and (d) R337Q mutant structures of HPA (thick lines). To facilitate comparisons, the structure of wild-type HPA (thin lines) has been overlaid on these drawings. The normally bound chloride ion in the wild-type enzyme (shown with an x) is absent in all mutant structures where, with the exception of the R337A HPA structure, this chloride ion is replaced by a water molecule. Water molecules bound in the vicinity of the chloride ion binding site of all structures are also indicated by an x. Also labeled are the three chloride ion binding site residues, R195, R337, and N298, as well as the three catalytic site residues, D197, E233 and D300, and H299.

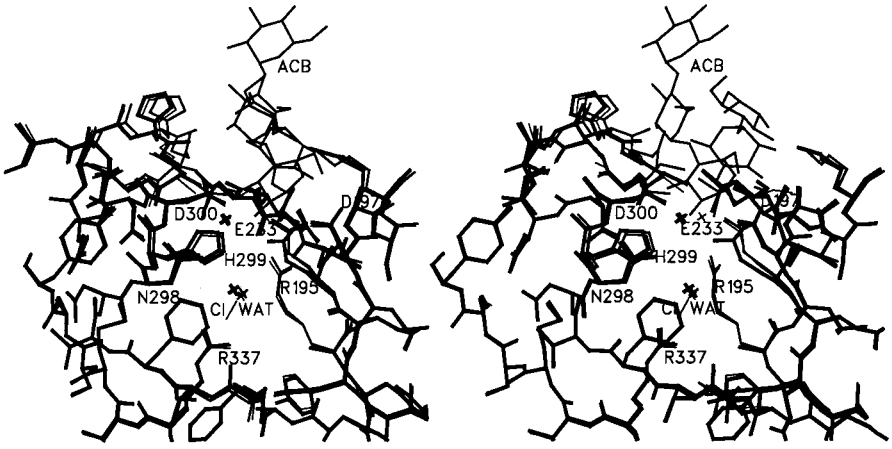

FIGURE 4: Stereo plot showing the close proximity of the chloride ion binding site to the active site of HPA as well as to the bound position of the inhibitor acarbose. Drawn are the structures of the chloride ion binding site and active sites of wild-type HPA (thin lines), an acarbose/HPA complex (medium lines), and the R195A mutant (thick lines). Chloride ion binding site residues, catalytic site residues, and bound acarbose (ACB) have been labeled. Bound chloride ion and water molecules are indicated with an x.

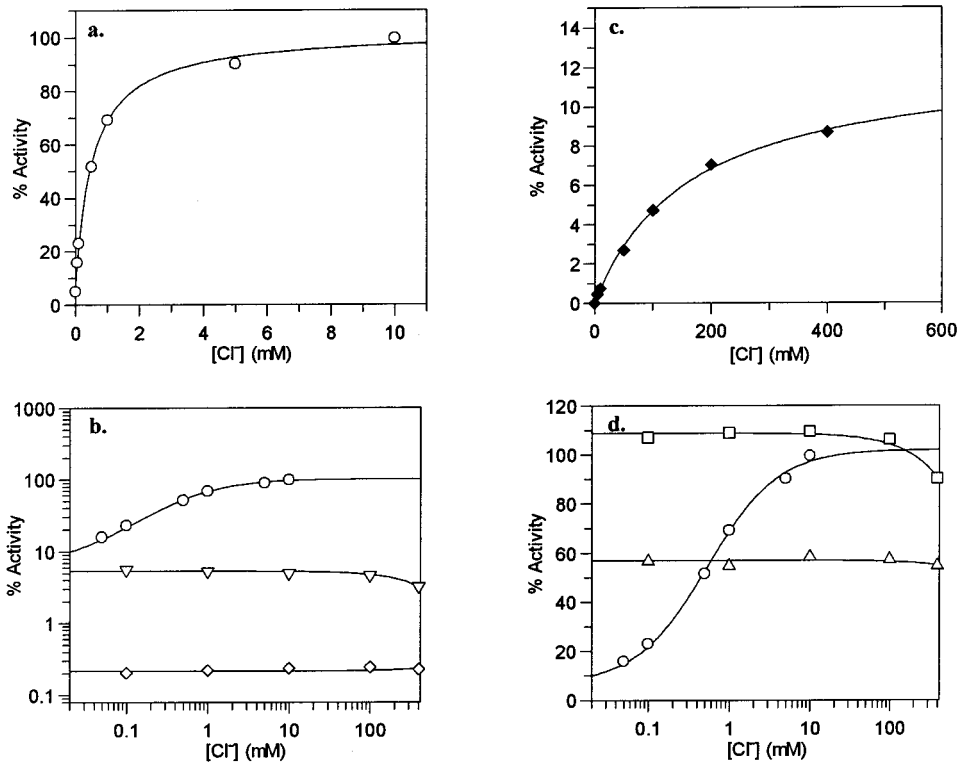

FIGURE 5: Dependence of (a) wild-type, (b) R195 mutant, (c) N298S mutant, and (d) R337 mutant enzymatic activities on chloride concentration: wild-type (○), R195A (◇), R195Q (▽), N298S (◆), R337A (△), and R337Q (□). Activities have been changed to percent activity for comparative purposes with wild-type HPA having 100% activity.

cupied normally by the chloride ion. Furthermore, the two water molecules observed in the active site of wild-type HPA are missing in the R337Q HPA structure.

Kinetic Studies of Wild-Type and Mutant HPAs

Wild-Type HPA. As was seen in the case of porcine pancreatic α-amylase (*21*) and *A. halioplanctis* α-amylase (*22*), the activity of wild-type HPA is dependent on chloride concentration in an approximately hyperbolic fashion (Figure 5a). α-Amylase activity increased 12-fold upon raising the chloride concentration from 0 to 10 mM. From these data, a K_d value of 0.53 ± 0.06 mM was determined for the binding of chloride to HPA. This value is comparable to the K_d value of 0.36 mM seen in the porcine counterpart (*21*). Furthermore, the value of K_d did not change when a shorter substrate (reduced maltohexaose) was used to measure the activity (data not shown), suggesting that the binding constant of chloride is independent of substrate size. Interestingly, at much higher concentrations of chloride (>400 mM), the enzyme seemed to be inhibited by the chloride in a concentration-dependent fashion. This effect was also seen in the mutants and may be due to a salt (ionic strength) effect at higher concentrations.

The dependence of wild-type HPA activity on pH was determined in the presence of a range of chloride concentrations, and a bell-shaped dependence (two ionization states) was observed at each of the chloride concentrations (Figure 6). Over the pH range used, the K_M of the enzyme toward

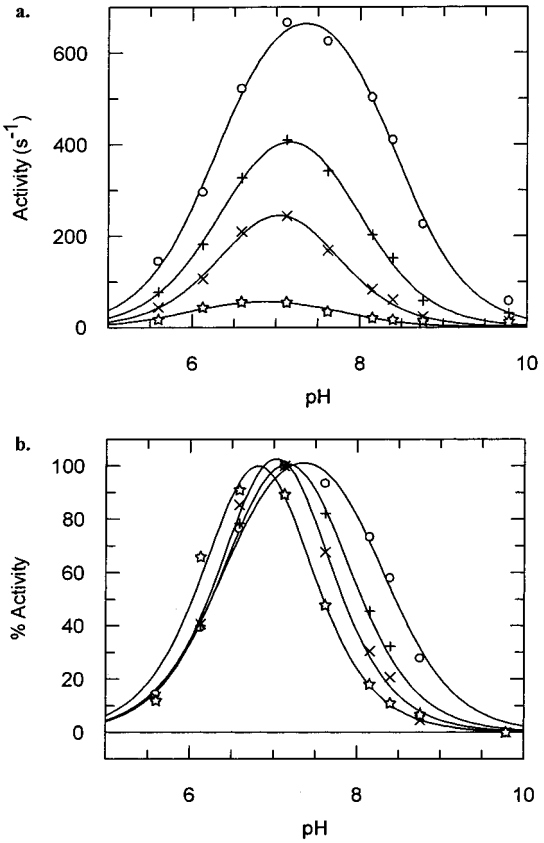

FIGURE 6: (a) pH profiles for the wild-type HPA activity at 0 mM (☆), 0.25 mM (×), 1 mM (+), and 100 mM (○) chloride concentration using starch as a substrate. (b) Normalized curves from the pH profiles of (a). The pK_{a1} (acidic limb) for the wild-type HPA at 100 mM NaCl was 6.4 compared to 6.4 for 0 mM NaCl. The pK_{a2} (basic limb) for the wild-type HPA at 100 mM NaCl was 8.3 compared to 7.2 for 0 mM NaCl.

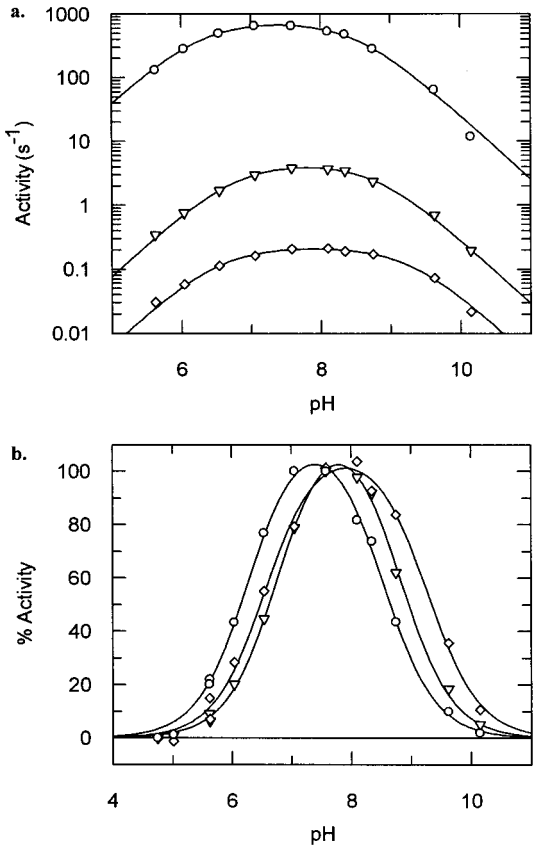

FIGURE 7: (a) pH profiles for the activities of the R195 mutants, R195A (◇) and R195Q (▽), in the absence of chloride. The pH profile of wild-type α-amylase in the presence of 100 mM chloride (○) is also plotted for comparative purposes. (b) Normalized curves from the pH profiles of (a). The pK_{a1} for the R195A and R195Q HPAs were 6.6 and 6.7, respectively. The pK_{a2} for R195A and R195Q HPAs were 9.2 and 8.8, respectively.

starch did not change significantly, and the activity was found to become maximal at starch concentrations beyond 1.0% (w/v). Therefore, these pH profiles are equivalent to a k_{cat} vs pH profile where the pK_a values reflect the ionizations in the ES complex. Comparison of the shape of the pH profile of the enzyme in the presence and absence of chloride revealed that the pK_a of the basic limb shifted to a lower value upon the removal of chloride (from 8.3 to 7.2). In contrast, the pK_a of the acidic limb seemed to stay constant at around pK_a 6.4.

R195 Mutant HPA. When the activities of the two R195 mutant HPAs were measured at varying chloride concentrations ranging from 0 to 100 mM, the activity was found to be independent of chloride concentration. At higher concentrations though, as with the wild-type enzyme, a decrease in activity was observed (Figure 5b). The activities of the R195A and R195Q HPAs compared to the wild-type HPA with chloride are lower by 450- and 20-fold, respectively. Furthermore, comparison of the pH profiles of the two mutant HPAs (Figure 7) with that of wild-type HPA in the presence of chloride revealed that the pK_a of the basic limb had shifted to a higher value: in the case of R195A HPA, it shifts from 8.3 to 9.2.

N298S HPA. When N298S HPA activity was measured at chloride concentrations ranging from 0 to 400 mM, the activity of the enzyme was found to depend on chloride concentration in a manner similar to that of the wild-type HPA (Figure 5c). However, the K_d value for the binding of chloride to the N298S HPA was determined to be 162 ± 13 mM. This is several orders of magnitude poorer binding than to the wild-type HPA. Furthermore, the maximal activity of this mutant HPA was 8-fold lower than that of wild-type HPA.

The dependence of N298S HPA activity on pH was determined in the presence of a range of concentrations of chloride, and a bell-shaped dependence was observed in each case (Figure 8). Comparison of the shapes of the pH profiles of the enzyme in the presence and absence of chloride revealed that the pK_a of the basic limb shifted to a lower value upon the reduction of chloride concentration by 100-fold (from 8.0 to 7.3). Unfortunately, in the complete absence of chloride the activity was too low to measure by the assay used in this study. Unlike the wild-type enzyme, however, the pK_a of the acidic limb also shifted to a lower pK_a value (from 6.5 to $<$5.1).

R337 Mutant HPAs. Measurement of enzymatic activity of the two R337 mutant proteins at varying chloride concentrations from 0 to 100 mM showed the activity to be independent of chloride concentration through this range (Figure 5d). This is consistent with results for the *A. halioplanctis* α-amylase where the activity of the K337A mutant protein was found to be independent of chloride concentration (*22*). However, in contrast to the *A. halioplanctis* enzyme where the mutation resulted in a significant

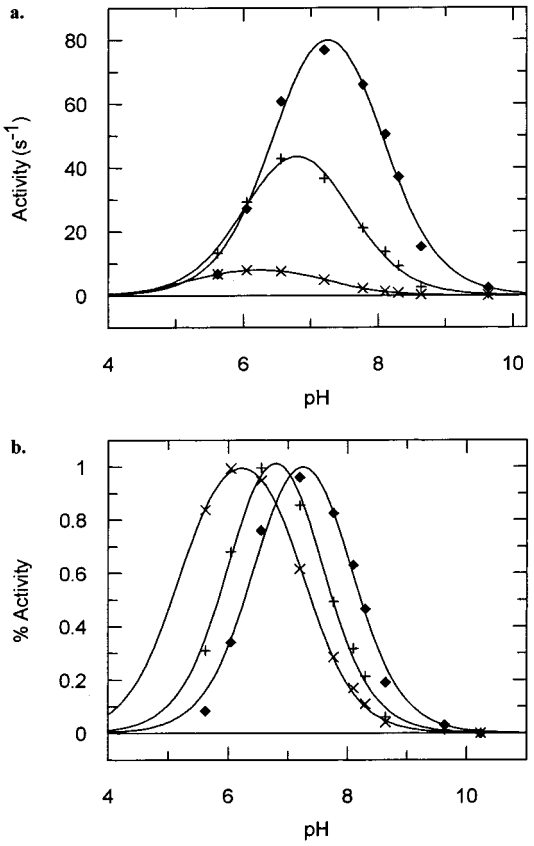

FIGURE 8: (a) pH profiles for the activity of the N298S mutant at 10 mM (×), 100 mM (+), and 400 mM (◆) chloride concentration using starch as a substrate. (b) Normalized curves from the pH profiles of (a). The pK_{a1} N298S HPA at 10 mM NaCl was 5.1 compared to 6.5 for 400 mM NaCl. The pK_{a2} for N298S HPA at 10 mM NaCl was 7.2 compared to 8.0 for 400 mM NaCl.

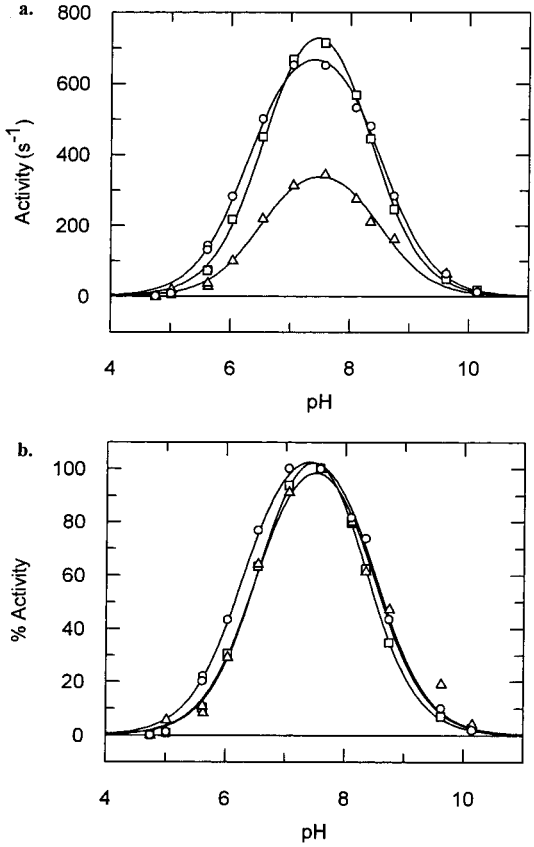

FIGURE 9: (a) pH profiles for the activities of the R337 mutants, R337A (△) and R337Q (□), in the absence of chloride. The pH profile of wild-type α-amylase in the presence of 100 mM chloride (○) is also plotted for comparative purposes. (b) Normalized curves from the pH profiles of (a). The pK_{a1} for the R337A and R337Q HPAs were 6.6 and 6.5, respectively. The pK_{a2} for R337A and R337Q HPAs were 8.5 and 8.3, respectively.

decrease in the enzyme activity (8-fold), the activity of R337A HPA is only 2-fold lower than that of the wild-type enzyme with chloride. Furthermore, our results showed that the R337Q mutant protein has enzymatic activity comparable to that of wild-type HPA in the presence of chloride.

The dependence of R337 mutant HPA activities on pH was determined in the absence of chloride, and a bell-shaped dependence was observed in each case (Figure 9). Notably, when the curves were normalized, it is clear that the pH dependences of the two R337 mutant enzymes in the absence of chloride are identical to that of the wild-type HPA in the presence of chloride. This pH profile did not change when the activities of the R337 mutant HPAs were measured in the presence of 100 mM chloride.

DISCUSSION

A comparison of the tertiary structures of the chloride ion binding sites of chloride-dependent α-amylases with the corresponding region in chloride-independent α-amylases reveals that the residue positions are surprisingly well conserved. The key difference between these two groups in this region is the side chain of residue 337. Although the main chain position of residue 337 is conserved throughout the α-amylase family, in the chloride-dependent group this residue is a basic amino acid (arginine or lysine) while in the chloride-independent group it is a nonbasic amino acid. In the chloride-dependent α-amylases, this basic residue seems to provide an essential coordinating ligand required for the creation of a chloride ion binding site. Consistent with this conclusion, all α-amylases without a basic residue at this position do not bind a chloride ion (*24*). The other arginine involved in the binding of the chloride ion is residue 195. This residue is conserved throughout the α-amylase family (*36*) and, from the crystal structure, seems to be involved in a number of roles in addition to that of chloride ion binding (*31*). Because the difference in chloride ion binding seems to lie in a single basic residue, removal of a coordinating arginine from the chloride-dependent HPA by mutation to a nonbasic residue might be expected to result in an α-amylase that does not bind a chloride ion. However, the effects expected on activity are less clear.

Indeed, structural analysis of the mutant HPAs, R195A, R195Q, R337A, and R337Q, crystallized in the presence of 5 mM NaCl showed no electron density for a bound chloride ion in any of these mutant proteins. By contrast, structures of wild-type HPA, with a K_d of 0.41 ± 0.06 mM for chloride, crystallized under the same conditions, consistently include a bound chloride ion. Kinetic analysis also suggests that chloride is not bound to any of these mutant HPAs. In the wild-type enzyme, the activity increases 12-fold upon increasing the chloride concentration from 0 to 10 mM. In contrast, no change on activity is seen for these mutant proteins when the chloride concentration is varied from 0 to 400 mM (Figure 5). These results clearly indicate the importance of R195 and R337 in binding the chloride ion

since removal of either coordinating ligand leads to a loss of the chloride ion binding site in HPA.

Conservation of the local structure of the chloride ion binding region in both chloride-dependent and -independent α-amylases suggests that the chloride ion is not responsible for stabilizing the general fold of this area. This is supported by earlier studies which showed by circular dichroism that the global folds of several chloride-dependent α-amylases were not affected by the absence of chloride (*21*, *22*). Consistent with this, the three-dimensional structures of the mutant HPAs, all of which are devoid of chloride ion, remain the same as that of wild-type HPA with chloride (Figure 3).

Surprisingly, the replacement of R195, which is intimately involved in a network of interactions, by either alanine or asparagine resulted in no significant structural changes to the active site residues to which it was directly hydrogen bonded in the wild-type HPA. This includes two key interactions to the catalytic residues D197 and E233 (Figure 2). These interactions could be expected to be responsible for orienting the active site residues into the optimal position. Structural studies of the two R195 mutant HPAs show that replacement of this residue results in only a minor reorientation of the carbonyl group of E233 (Figure 3a,b). The replacement of R337, which in turn resulted in the loss of the chloride ion, did not even result in this change (Figure 3c,d). These results suggest that the binding of the chloride ion does not result in local structural changes, as had been suggested may be the case from previous studies (*21*, *22*). Instead, the activity changes that result from the removal of the chloride can most likely be attributed to electrostatic changes introduced into the local environment of the active site.

While the role of the chloride ion binding site residues is not made clear by the structural studies, kinetic studies decisively revealed their importance. Comparison of the activities of the R195 mutant HPAs with that of the wild-type HPA in the presence of chloride, using starch as substrate, revealed dramatic lowering of activities for both R195A and R195Q HPAs (Figure 5b). Although this may be an effect of slight misalignments of the active site residues, there are several other factors that may be of more importance. In particular, as can be seen in Figure 2, R195 forms a hydrogen bond to the 2-hydroxyl of the substrate sugar moiety bound in the −1 binding subsite. It has been shown previously in other glycosidases (*18*) that very important interactions form between the enzyme and the 2-hydroxyl at the transition state. Thus, the removal of any such interactions may compromise catalysis. The same may be true in the α-amylase family; thus, one of the roles of R195 may be to provide significant stabilization to the transition state during catalysis by stabilizing the position of the 2-hydroxyl.

The pH profiles for the R195 mutant HPAs reveal that the pK_a values of both the acidic limb and basic limb shift to a higher value (Figure 7). According to the double displacement mechanism (Figure 1), the acid/base catalyst needs to be protonated in the first step in order to provide catalysis. Therefore, the basic limb of the pH profile most likely reflects the protonation state of E233 (catalytic acid/base). By the same reasoning, the acidic limb of the profile would be expected to reflect the protonation state of D197 (catalytic nucleophile). Indeed, this has been unequivocally demonstrated for another glycosidase, the *Bacillus circulans* β-xylanase, using ^{13}C NMR (*37*). Removal of the positively charged R195 side chain in HPA might be expected to raise the pK_a value of the adjacent catalytic residues (D197 and E233), making them less prone to protonation (*38*). However, the removal of this side chain also results in the loss of the chloride ion and its negative charge, which is also in the vicinity of the active site. This effect would therefore counter, to some extent, the consequences of removal of the arginine. Thus, the resulting pK_a shifts are relatively modest in contrast to what might otherwise have been expected from removal of the arginine alone.

Comparisons of the pH profiles of wild-type HPA (in the presence of chloride) with those of the R337 mutant HPAs reveal that no significant shifts have occurred either in the acidic or basic pK_a values (Figure 9). Furthermore, and most surprisingly, the activities of the two mutant HPAs are very similar to that of the wild-type enzyme (in the presence of chloride). To reiterate, in the case of the wild-type enzyme, increasing the concentration of chloride increases the activity of the enzyme at pH 6.9 (Figure 5a). In addition, this increase in chloride concentration is also associated with a shift of the pH optimum to a more basic pH. In the case of the R337 mutants, the enzyme activity is independent of chloride concentration with kinetic parameters very similar to those of wild-type HPA in the presence of chloride. These data therefore indicate that the effects of a replacement at R337 are being counteracted by the loss of the chloride.

This surprising result can be explained if the role of the mechanism of chloride activation involves neutralization of the positive charge from the side chain of R337 that would otherwise affect the pK_a of E233 (catalytic acid/base). In wild-type HPA, the side chain of R337 is located ∼8 Å away from the carbonyl group of E233 and, aside from the chloride ion, no residue spatially intervenes between these two residues. Thus, when no chloride ion is present, the positive charge on R337 might be expected to shift the pK_a of E233 to a lower value through electrostatic interactions as indeed is seen for wild-type HPA. Inclusion of chloride raises the pK_a of E233 to 8.3 via charge screening.

The pH profile for the wild-type HPA suggests that the effect of the chloride on the pK_a of E233 is more significant than its effect on the pK_a of D197. Indeed, the structural data show that D197 is "shielded" from the direct effects of R337 by R195. In this case, as the chloride concentration is reduced, the pK_a of the basic limb of the pH profile will be lowered while the pK_a of the acidic limb will stay around the same. As these two pK_as get closer in value, the pH profiles for each of the two residues start overlapping with a resultant overall reduction in enzymatic activity. With the removal of the R337 side chain, the positive charge is no longer present. Therefore, even though the chloride ion does not bind, the R337 mutant HPAs have kinetic properties similar to those of the wild-type enzyme with chloride.

The final coordination ligand in the chloride ion binding site is N298. Because this residue is not charged and only provides one point of interaction, replacement of the asparagine with a serine was not expected to completely destroy the binding site. Consistent with this expectation, the activity of N298S HPA, although lower, was still found to be dependent on chloride concentration although the binding constant for chloride worsened by 3 orders of magnitude

(Figure 5c). More importantly, the pK_a shifts that were observed when reducing the concentration of chloride in wild-type HPA were also seen in this mutant enzyme. This seems to imply that N298 is acting to increase the chloride ion binding ability but that it does not directly participate in the mechanism of chloride activation.

Although these mutations shed some light on the mechanism of chloride activation in HPA, they do not shed much light on the possible reason for the presence of this chloride ion binding site in HPA. In a recent review, D'Amico et al. (*24*) listed a number of sources of chloride-dependent amylases. This list, although consisting primarily of mammals, also included insects and bacteria, suggesting that, possibly, this chloride ion binding site may have been introduced early in evolution. With chloride being ubiquitous throughout nature, there may not have been a selective pressure to mutate the R337 residue to a nonbasic amino acid. Interestingly, in another chloride-dependent enzyme, human angiotensin I converting enzyme, the chloride dependence has been associated with a change in substrate specificity (*39*). In the case of HPA, however, this kind of a change has not been observed.

In summary, therefore, the chloride ion binding site contains three key amino acids: R195, N298, and R337. In addition to helping form the chloride ion binding site, R195 also plays other key roles in orienting the two carboxylic acids and probably helping to set their pK_a values, as well as providing hydrogen-bonding interactions to the substrate 2-hydroxyl. N298 plays a role in increasing the affinity of the chloride ion binding site toward chloride but also seems to be important in interacting with the active site residues to aid in catalysis. Consistent with these key roles, these residues are almost fully conserved in both the chloride-dependent and chloride-independent α-amylases, and the mutation of these residues has catastrophic kinetic consequences. R337, on the other hand, appears to function almost as an intramolecular inhibitor of the enzyme, but an inhibitor whose effect can be opposed by the binding of chloride.

ACKNOWLEDGMENT

We thank Dr. D. G. Kilburn for the generous gift of the endoglycosidase F−cellulose binding domain fusion protein and Dr. Shouming He for obtaining the mass spectra.

REFERENCES

1. Thoma, J., Spradlin, J., and Dygert, S. (1971) in *The Enzymes* (Boyer, P., Ed.) pp 115−189, Academic Press, New York.
2. Vihinen, M., and Mantsala, P. (1989) *Crit. Rev. Biochem. Mol. Biol. 24*, 329−418.
3. Henrissat, B. (1991) *Biochem. J. 280*, 309−316.
4. Henrissat, B., and Bairoch, A. (1993) *Biochem. J. 293*, 781−788.
5. Henrissat, B., and Bairoch, A. (1996) *Biochem. J. 316*, 695−696.
6. Henrissat, B. (1998) *Biochem. Soc. Trans. 26*, 153−156.
7. Aghajari, N., Feller, G., Gerday, C., and Haser, R. (1998) *Protein Sci. 7*, 564−572.
8. Brzozowski, A. M., and Davies, G. J. (1997) *Biochemistry 36*, 10837−10845.
9. Boel, E., Brady, L., Brzozowski, A. M., Derewenda, Z., Dodson, G. G., Jensen, V. J., Petersen, S. B., Swift, H., Thim, L., and Woldike, H. F. (1990) *Biochemistry 29*, 6244−6249.
10. Machius, M., Wiegand, G., and Huber, R. (1995) *J. Mol. Biol. 246*, 545−559.
11. Kadziola, A., Abe, J., Svensson, B., and Haser, R. (1994) *J. Mol. Biol. 239*, 104−121.
12. Buisson, G., Duee, E., Haser, R., and Payan, F. (1987) *EMBO J. 6*, 3909−3916.
13. Ramasubbu, N., Paloth, V., Luo, Y. G., Brayer, G. D., and Levine, M. J. (1996) *Acta Crystallogr. D52*, 435−446.
14. Brayer, G. D., Luo, Y., and Withers, S. G. (1995) *Protein Sci. 4*, 1730−1742.
15. Tao, B. Y., Reilly, P. J., and Robyt, J. F. (1989) *Biochim. Biophys. Acta 995*, 214−220.
16. Rydberg, E. H., Sidhu, G., Vo, H. C., Hewitt, J., Cote, H. C., Wang, Y., Numao, S., MacGillivray, R. T., Overall, C. M., Brayer, G. D., and Withers, S. G. (1999) *Protein Sci. 8*, 635−643.
17. Uitdehaag, J. C., Mosi, R., Kalk, K. H., van der Veen, B. A., Dijkhuizen, L., Withers, S. G., and Dijkstra, B. W. (1999) *Nat. Struct. Biol. 6*, 432−436.
18. Ly, H. D., and Withers, S. G. (1999) *Annu. Rev. Biochem. 68*, 487−522.
19. Koshland, D. E. (1953) *Biol. Rev. 28*, 416−436.
20. Sinnott, M. L. (1990) *Chem. Rev. 90*, 1171−1202.
21. Levitzki, A., and Steer, M. L. (1974) *Eur. J. Biochem. 41*, 171−180.
22. Feller, G., Bussy, O., Houssier, C., and Gerday, C. (1996) *J. Biol. Chem. 271*, 23836−23841.
23. Wakim, J., Robinson, M., and Thoma, J. A. (1969) *Carbohydr. Res. 10*, 487−503.
24. D'Amico, S., Gerday, C., and Feller, G. (2000) *Gene 253*, 95−105.
25. Taylor, R. H., Jenkins, D. J., Barker, H. M., Fielden, H., Goff, D. V., Misiewicz, J. J., Lee, D. A., Allen, H. B., MacDonald, G., and Wallrabe, H. (1982) *Diabetes Care 5*, 92−96.
26. Jenkins, D. J., Taylor, R. H., Goff, D. V., Fielden, H., Misiewicz, J. J., Sarson, D. L., Bloom, S. R., and Alberti, K. G. (1981) *Diabetes 30*, 951−954.
27. Meyer, B. H., Muller, F. O., Kruger, J. B., Clur, B. K., and Grigoleit, H. G. (1984) *S. Afr. Med. J. 66*, 222−223.
28. Sambrook, J., Fritsch, E. F., and Maniatis, T. (1989) *Molecular Cloning: A Laboratory Manual*, Cold Spring Harbor Laboratory, Cold Spring Harbor, NY.
29. Bernfeld, P. (1955) *Methods Enzymol. 1*, 149−158.
30. Leatherbarrow, R. J. (1998) Erithacus Software Ltd., Staines, U.K.
31. Brayer, G. D., Sidhu, G., Maurus, R., Rydberg, E. H., Braun, C., Wang, Y. L., Nguyen, N. T., Overall, C. M., and Withers, S. G. (2000) *Biochemistry 39*, 4778−4791.
32. Otwinowski, Z., and Minor, W. (1997) *Methods Enzymol. 276*, 307−326.
33. Brünger, A. T. (1992) *X-PLOR: A system for X-ray crystallography and NMR*, Yale University Press, New Haven, CT.
34. Jones, T. A., Zhou, J.-Y., Cowan, S. W., and Kjeldgaard, M. (1991) *Acta Crystallogr. A47*, 110−119.
35. Luzzati, P. V. (1952) *Acta Crystallogr. 5*, 803−810.
36. MacGregor, E. A. (1988) *J. Protein Chem. 7*, 399−415.
37. McIntosh, L. P., Hand, G., Johnson, P. E., Joshi, M. D., Korner, M., Plesniak, L. A., Ziser, L., Wakarchuk, W. W., and Withers, S. G. (1996) *Biochemistry 35*, 9958−9966.
38. Joshi, M. D., Sidhu, G., Pot, I., Brayer, G. D., Withers, S. G., and McIntosh, L. P. (2000) *J. Mol. Biol. 299*, 255−279.
39. Liu, X. F., Fernandez, M., Wouters, M. A., Heyberger, S., and Husain, A. (2001) *J. Biol. Chem. 276*, 33518−33525.

BI0115636